Thermochimica Acta, 21 (1977) 273–284

INFLUENCE OF TEMPERATURES AND STARTING MATERIALS USED TO PREPARE α-Fe_2O_3 ON ITS CATALYTIC ACTIVITY AT THE THERMAL DECOMPOSITION OF $KClO_4$

M. SHIMOKAWABE, R. FURUICHI AND T. ISHII
Department of Applied Chemistry, Faculty of Engineering, Hokkaido University, Sapporo, 060 (Japan)
(Received 20 December 1976)

ABSTRACT

In order to elucidate the influence of preparative history of α-Fe_2O_3 on its reactivity, the catalytic thermal decomposition of $KClO_4$ by α-Fe_2O_3 was studied by means of DTA and X-ray techniques. The catalysts were prepared by the calcination of three iron salts, $Fe(OH)(CH_3COO)_2$, $FeSO_4 \cdot 7H_2O$ and $Fe_2(SO_4)_3 \cdot xH_2O$, at temperatures of 500–1200°C in air. The lower the preparation temperature of α-Fe_2O_3, the larger the specific surface area and reversely the smaller the crystalline size. $KClO_4$ without α-Fe_2O_3 was found to begin fusion and decomposition simultaneously at about 530°C. The addition of α-Fe_2O_3 resulted in promotion of the decomposition reaction of $KClO_4$; a lowering of 30–110°C in the initial decomposition temperature and a solid-phase decomposition before fusion of $KClO_4$. The influence of preparative history of α-Fe_2O_3 on the decomposition mainly depended on the preparation temperature rather than the starting material. The initial decomposition temperature of $KClO_4$ increased with an increase of the preparation temperature of α-Fe_2O_3. The effect of α-Fe_2O_3 was discussed on the basis of the charge transfer and the oxygen abstraction models.

INTRODUCTION

α-Fe_2O_3 is widely used in industry, e.g., as a raw material for the synthesis of ferrite, a catalyst for oxidation reactions, a source of pigment, etc. The physicochemical properties of α-Fe_2O_3 have been found to vary remarkably with its method of preparation histories, such as the kind of starting iron salts, the preparation temperatures, the preparation atmospheres and the addition of foreign ions. Gallagher et al.[1] studied the reactivity of twelve α-Fe_2O_3, which were prepared by the decomposition of various iron salts, by using the reactions of $LiFeO_2$ formation and dissolution in HCl-solution. They observed that the lowest decomposition temperature of each iron salt leads to the highest reactivity of α-Fe_2O_3 which has a large specific surface area, a low density and a small particle size. Gallagher et al. concluded that the high defect concentration and the low crystallinity of the oxide cause the high reactivity. Several investigators[2-4] have also studied the reactivity of α-Fe_2O_3 prepared at different temperatures by using the synthesis reactions of $CdFe_2O_4^2$ and $ZnFe_2O_4^3$, and the catalytic decompositions of $H_2O_2^2$ and CH_3OH^4. The results were interpreted on the basis of defect structure and lattice disorder of the oxide.

On the other hand, it has been reported[5-10] that the metal oxides catalytically promote the thermal decomposition of $KClO_4$ to cause a lowering of the decomposition temperature. Recently, authors reported[11] that the transition metal oxides, such as α-Fe_2O_3, Cr_2O_3 and MnO_2, markedly accelerate the thermal decomposition of $KClO_4$; these oxides caused a lowering of 100–200°C in the initial decomposition temperature (T_i) and a solid-phase decomposition of $KClO_4$. The pronounced effect of these oxides was explained by the electron transfer mechanism[6, 8] and the oxygen abstraction model[7].

In this work, in order to investigate the influence of preparative history of α-Fe_2O_3 on its reactivity, the oxides were prepared by calcination of three iron salts at different temperatures and their reactivity for the catalytic thermal decomposition of $KClO_4$ was investigated by means of DTA and X-ray techniques.

EXPERIMENTAL

Materials

Three iron salts shown in Table 1 were used as the starting materials. α-Fe_2O_3(A) was prepared by calcination of $Fe(OH)(CH_3COO)_2$(Kanto) in a stream of air (100 ml min^{-1}) at temperatures of 500–1200°C for 1 h. α-$Fe_2O_3(S_1)$ and α-$Fe_2O_3(S_2)$ were prepared by dehydration of $FeSO_4 \cdot 7H_2O$ and $Fe_2(SO_4)_3 \cdot xH_2O$(Kanto), respectively, in air at 200°C for 30 min and subsequent calcination in a stream of air at temperatures of 700–1200°C for 1 h. These samples were abbreviated as follows. For example, the sample prepared by the calcination of $FeSO_4 \cdot 7H_2O$ at 700°C was indicated in such a form as α-$Fe_2O_3(S_1$-700). In order to remove residual sulfate ions in α-$Fe_2O_3(S_1)$ and α-$Fe_2O_3(S_2)$, the samples were washed with hot water until no $BaSO_4$ precipitate was observed in the filtrate. After washing, the samples were

TABLE 1

IRON SALTS USED AS STARTING MATERIAL

Sample	*Iron salt*
α-Fe_2O_3(A)	Basic ferric acetate $Fe(OH)(CH_3COO)_2$
α-$Fe_2O_3(S_1)$	Ferrous sulfate hydrate $FeSO_4 \cdot 7H_2O$
α-$Fe_2O_3(S_2)$	Ferric sulfate hydrate $Fe_2(SO_4)_3 \cdot xH_2O$

dried in air at 110°C for 8 h. Infrared spectra of washed samples did not show absorption peaks of SO_4^{2-} (ν = 983,1105 cm^{-1}). All iron oxides prepared were confirmed to be α-Fe_2O_3 by X-ray diffraction patterns. $KClO_4$ used in the experiments was GR reagent from Kanto Chemical Co. All samples were ground to pass 200 mesh sieve. Samples for DTA and TG experiments were obtained by mixing $KClO_4$ with α-Fe_2O_3 (weight ratio = 1 : 1) in an agate mortal for 20 min.

DTA, TG and X-ray diffraction

Apparatus and experimental conditions employed were the same as previously described[10, 11]. DTA and TG experiments were carried out at a heating rate of 5°C min^{-1} in air atmosphere.

The initial decomposition temperature (T_i)

The value of T_i for $KClO_4$–α-Fe_2O_3 mixtures was determined by measuring the onset temperature of exothermic deflection of the DTA curve, and confirmed by the existence of the decomposition product(KCl) in the X-ray diffraction pattern of DTA sample heated to the onset temperature. The accuracy of T_i was ± 5°C.

Specific surface area

The specific surface area of α-Fe_2O_3 was estimated by the BET method[12, 13] from the amount of N_2 adsorbed at liquid nitrogen temperature. 16.2 $Å^2$ was employed as the cross-sectional area of N_2.

Crystalline size

The crystalline size of α-Fe_2O_3 was estimated by the X-ray diffraction method[14, 15]. NaCl was used as the reference material.

RESULTS

Thermal decomposition of $KClO_4$

Figures 1(A)–(C) show DTA and TG curves of $KClO_4$, and X-ray diffraction patterns of partially decomposed $KClO_4$. In the DTA curve, ΔT is expressed in μV scale of chromel–alumel thermocouple. DTA curve(A) shows two endothermic peaks at 310 and 570°C and an exothermic peak at 600°C. These three peaks correspond with the solid-phase transition from the rhombic to the cubic form, the fusion of solid $KClO_4$ and the exothermic decomposition in the liquid state, respectively. It is found from TG curve(B) that the decrease in weight corresponding to the decomposition ($KClO_4 \rightarrow KCl + O_2$) begins at about 530°C. X-ray diffraction patterns(C) show that the presence of the decomposition product (KCl) is identified in the DTA sample at the temperature (550°C) immediately after the beginning of fusion. From the facts mentioned above, it is found that the fusion and the decomposition take place simultaneously in the case of $KClO_4$ alone. Therefore, the endothermic DTA peak at 570°C is regarded as the result of the overlap of fusion with decomposition. For the

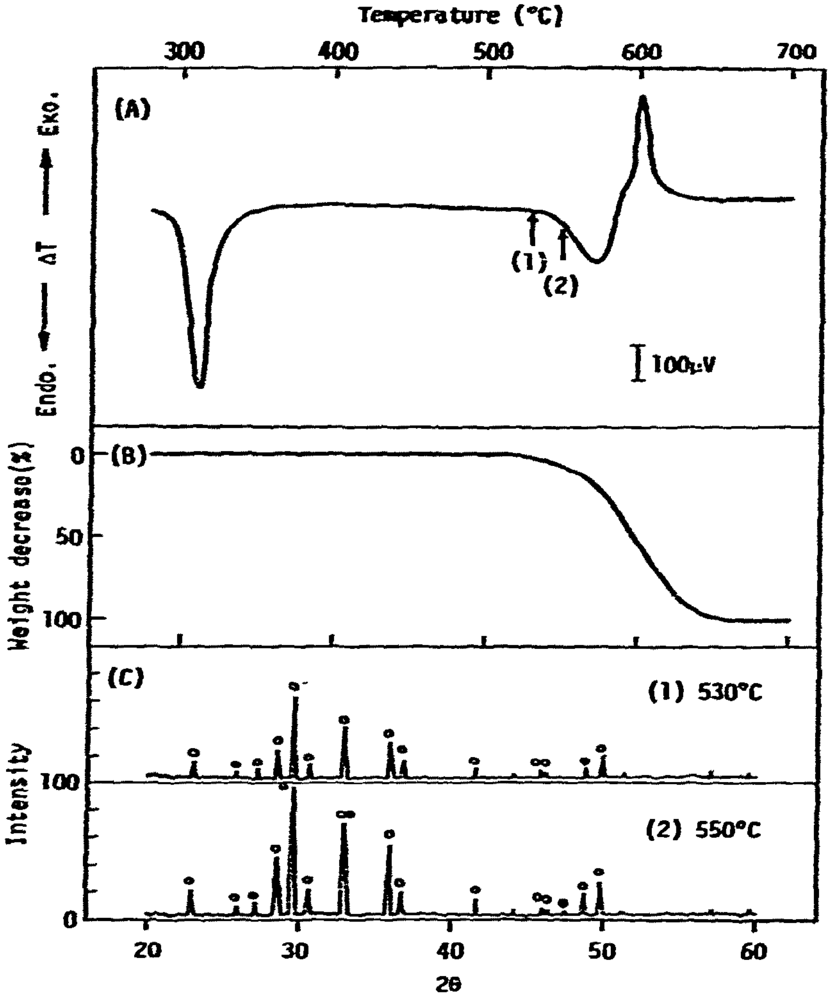

Fig. 1. (A) DTA; and (B) TG curves of $KClO_4$; and (C) X-ray diffraction patterns of samples at temperatures shown by arrows on DTA curve. ○, $KClO_4$; ●, KCl.

sake of convenience in this paper, however, two peaks at 570 and 600 °C are termed the fusion peak and the decomposition peak, respectively. It has been reported[16–19] that the thermal decomposition of $KClO_4$ proceeds through $KClO_3$ as an intermediate product to form KCl and oxygen.

$$KClO_4 \rightarrow KClO_3 + 1/2O_2 \quad (1)$$

$$KClO_3 \rightarrow KCl + 3/2O_2 \quad (2)$$

In the present experiments, however, the presence of $KClO_3$ was not identified from TG and X-ray diffraction patterns.

Effect of α-Fe_2O_3 additives on the thermal decomposition of $KClO_4$

Table 2 shows the effect of the mixing ratio on the DTA peak temperature of

TABLE 2

EFFECT OF THE MIXING RATIO OF $KClO_4$ AND α-Fe_2O_3 ON THE PEAK TEMPERATURES OF THE TRANSITION, THE FUSION AND THE DECOMPOSITION OF $KClO_4$

Composition of mixture (g)		*Peak temperature (°C)*		
$KClO_4$	*α-Fe_2O_3**	*Transition*	*Fusion*	*Decomposition*
1.00	0	312	574	600
0.90	0.10	311	528	536
0.80	0.20	312	522	529
0.70	0.30	311	518	525
0.60	0.40	310	513	522
0.50	0.50	308	511	518

* Prepared by the calcination of $Fe_2(SO_4)_3 \cdot xH_2O$ in a stream of air at 800°C for 4.5 hr.

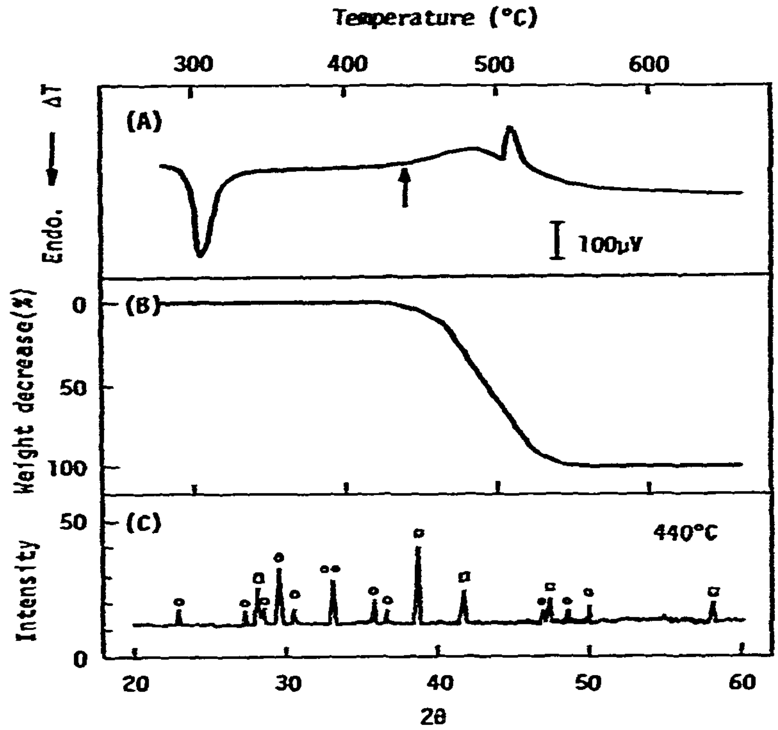

Fig. 2. (A) DTA; and (B) TG curves of $KClO_4$ with α-$Fe_2O_3(S_1$-700); and (C) X-ray diffraction patterns of sample at the temperature shown by the arrow on the DTA curve. ○, $KClO_4$; ●, KCl; □, α-Fe_2O_3.

$KClO_4$–α-$Fe_2O_3(S_2$-800) systems. The peak temperatures of fusion and decomposition decrease with an increase in the α-$Fe_2O_3/KClO_4$ ratio. On the other hand, the addition of α-Fe_2O_3 has little effect on the solid-phase transition of $KClO_4$. In cases when less than 0.4g of α-Fe_2O_3 was added, the molten $KClO_4$ flew down from the sample holder which was placed in vertical position. Consequently in all experiments, $KClO_4$ and α-Fe_2O_3 were mixed at a ratio of 0.5g : 0.5g.

Figures 2(A)–(C) show DTA and TG curves of $KClO_4$ with α-Fe_2O_3 (S_1-700), and the X-ray diffraction pattern of the partially decomposed $KClO_4$ sample. A remarkable effect of the α-Fe_2O_3 additive on the DTA curve for the thermal decom-

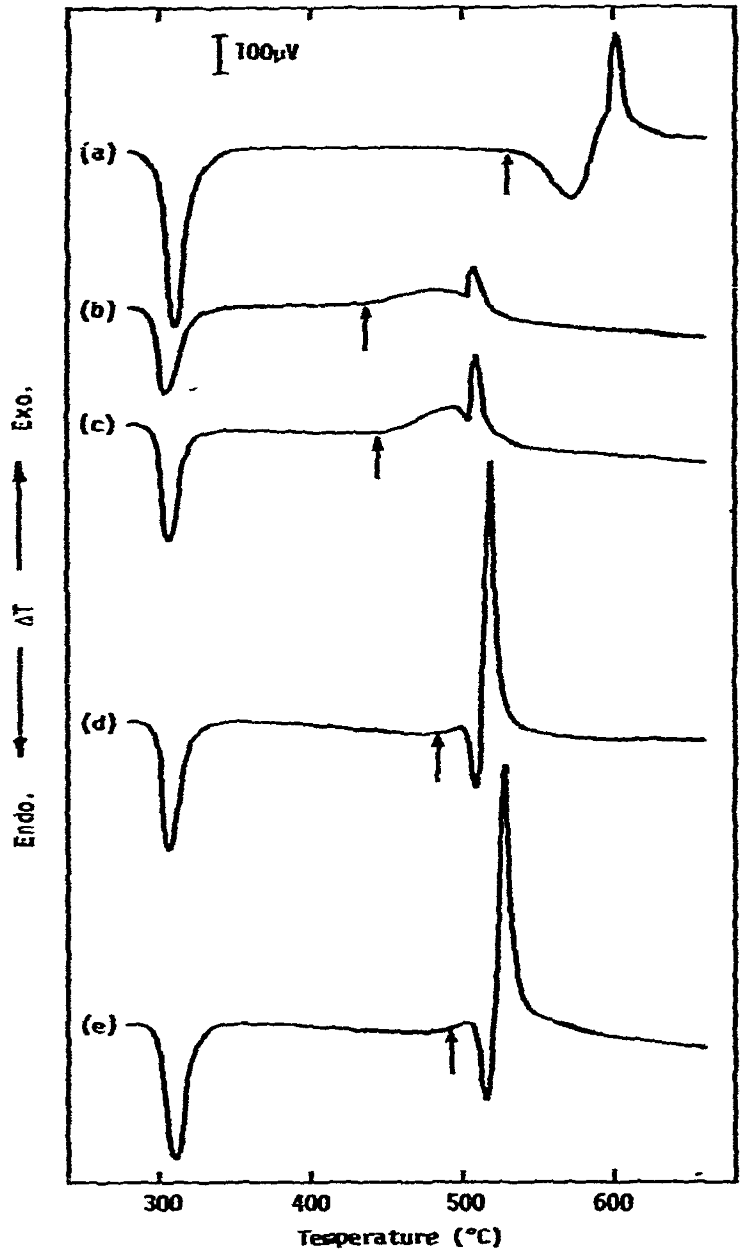

Fig. 3. DTA curves of $KClO_4$ with α-Fe_2O_3 prepared by calcination of $FeSO_4 \cdot 7\,H_2O$ in air. (a) $KClO_4$; (b) $KClO_4$ + α-Fe_2O_3(S_1-700); (c) $KClO_4$ + α-Fe_2O_3(S_1-800); (d) $KClO_4$ + α-Fe_2O_3 (S_1-900); (e) $KClO_4$ + α-Fe_2O_3(S_1-1100). ↑ = Initial decomposition temperature (T_i).

position is observed by comparing Fig. 2A with Fig. 1A. The exothermic reaction is initiated at about 435°C before the beginning of the fusion of $KClO_4$. TG curve(B) of the same sample shows that the decrease in weight begins at the same temperature as that at the onset of the exothermic peak of DTA (curve(A). The sample heated to 440°C shown by the arrow on DTA curve(A) indicated no symptom of fusion, and the X-ray diffraction pattern(C) of this sample showed the presence of KCl. Accordingly, the exothermic DTA peak of $KClO_4$ with α-Fe_2O_3 seems to be due to the solid-phase thermal decomposition before the fusion.

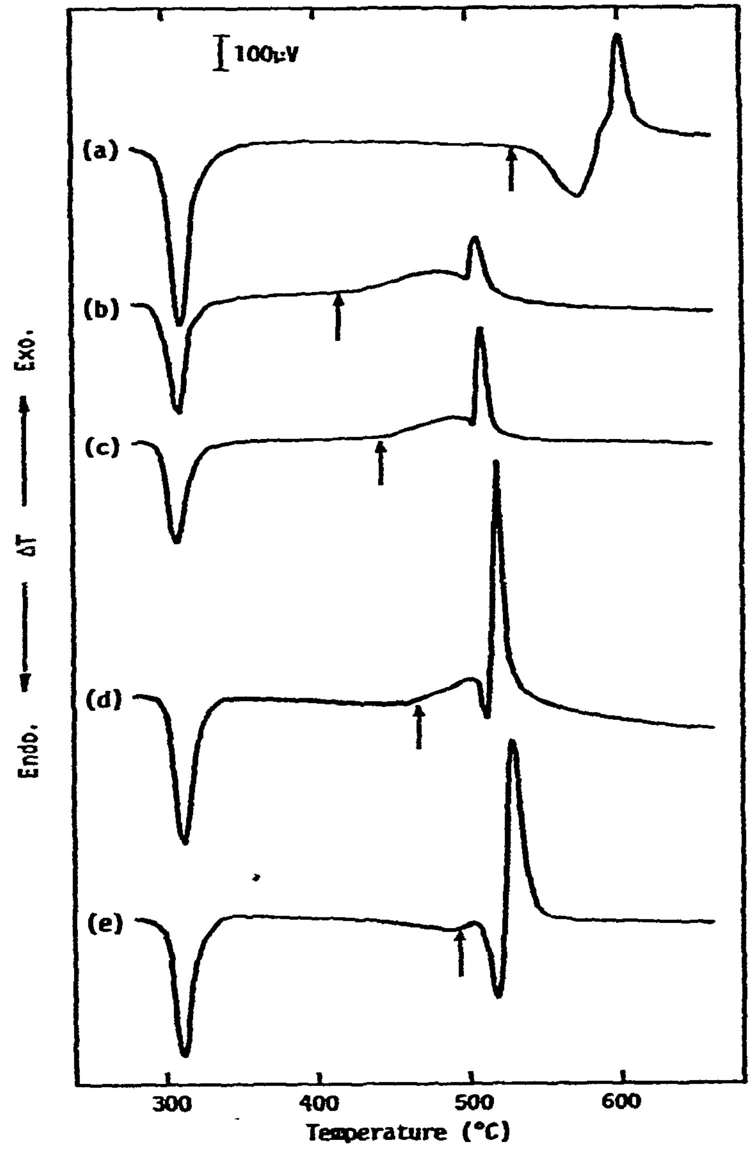

Fig. 4. DTA curves of $KClO_4$ with α-Fe_2O_3 prepared by calcination of $Fe(OH)(CH_3COO)_2$ in air. (a) $KClO_4$; (b) $KClO_4$ + α-Fe_2O_3(A-500); (c) $KClO_4$ + α-Fe_2O_3(A-700); (d) $KClO_4$ + α-Fe_2O_3 (A-900); (e) $KClO_4$ + α-Fe_2O_3(A-1200). ↑ = Initial decomposition temperature (Ti).

Influence of the preparative history of α-Fe_2O_3 additives on the thermal decomposition of $KClO_4$

The initial decomposition temperature (T_i) of $KClO_4$ was employed as a measure to indicate the reactivity of α-Fe_2O_3 with a different preparative history. The specific surface area and the crystalline size of α-Fe_2O_3 were also measured in order to be able to discuss the relationship between its preparative history and its reactivity. The lowest preparing temperature of α-Fe_2O_3 was determined by measuring the lowest temperature of decomposition of each iron salt to α-Fe_2O_3, using DTA and X-ray techniques; 500, 700 and 700°C for $Fe(OH)(CH_3COO)_2$, $FeSO_4 \cdot 7H_2O$ and $Fe_2(SO_4)_3 \cdot xH_2O$, respectively. These three iron salts are chosen to compare the influence of differences in anion and in valence of cation.

Figure 3 shows DTA curves of $KClO_4$-α-$Fe_2O_3(S_1)$ systems. Curve(a) and curves (b, c, d and e) correspond to pure $KClO_4$ and $KClO_4$ with α-$Fe_2O_3(S_1)$ prepared at 700, 800, 900 and 1100°C, respectively. The arrow on each curve indicates

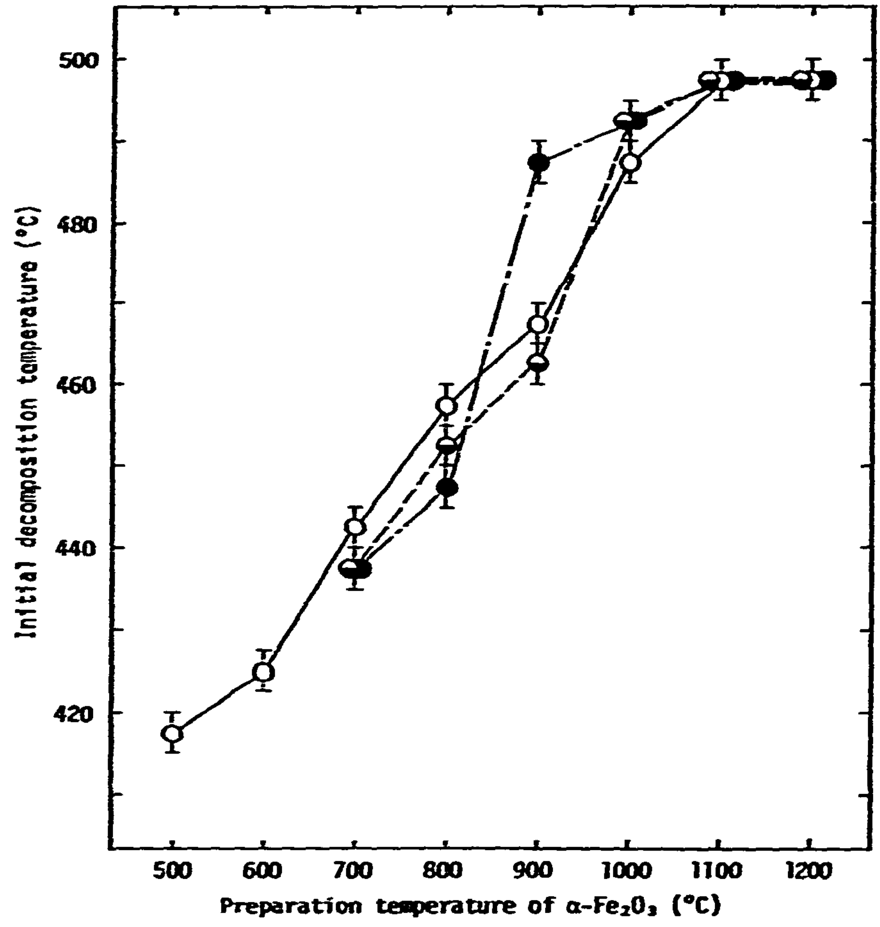

Fig. 5. Relation between initial decomposition temperature (T_i) of $KClO_4$ and preparation temperature of α-Fe_2O_3. ○, α-Fe_2O_3(A); ●, α-$Fe_2O_3(S_1)$; ◒, α-$Fe_2O_3(S_2)$.

the initial decomposition temperature (T_i) of $KClO_4$. T_i of pure $KClO_4$, curve (a), is 530–550°C. On the other hand, all α-Fe_2O_3 additives cause the exothermic reaction before the fusion of the salt and the lowering of T_i (curve (b)–(e)). The lower the preparation temperature of α-Fe_2O_3, the lower T_i and the smaller the exothermic peak of the molten-phase decomposition occurring after the fusion peak. The α-Fe_2O_3 additives have little effect on the solid-phase transition peak at 310°C.

Figure 4 shows the DTA curves of $KClO_4$–α-Fe_2O_3(A) systems. Curve (a) and curves (b, c, d and e) correspond to pure $KClO_4$ and $KClO_4$ with α-Fe_2O_3(A) prepared at 500, 700, 900 and 1200°C, respectively. In the same manner as seen in Fig. 3, α-Fe_2O_3 additives cause remarkable lowering of T_i and the solid-phase decomposition.

Figure 5 shows the relation between the preparation temperature of α-Fe_2O_3 and T_i of $KClO_4$–α-Fe_2O_3 systems. It is found that the value of T_i does not depend

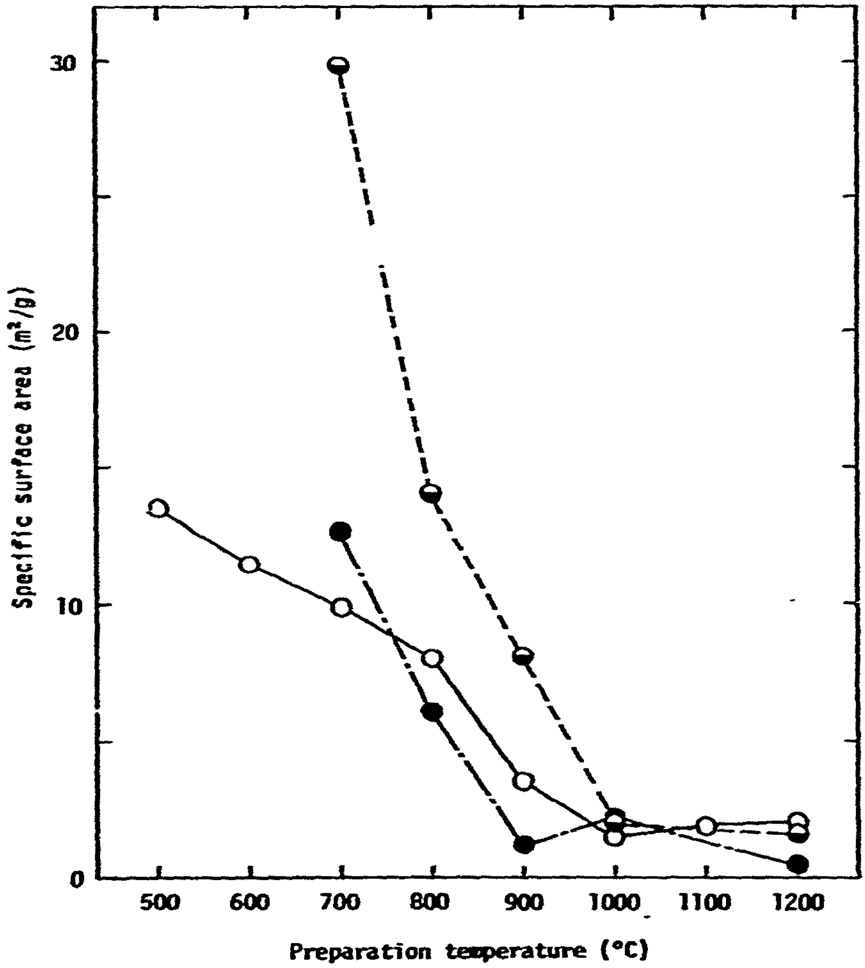

Fig. 6. Relation between specific surface area and preparation temperature of α-Fe_2O_3. ○, α-Fe_2O_3 (A); ●, α-$Fe_2O_3(S_1)$; ⊖, α-$Fe_2O_3(S_2)$.

on which starting iron salt was used for the preparation of α-Fe_2O_3, T_i increases almost linearly with increasing preparation temperature of α-Fe_2O_3 up to 1100°C, and α-Fe_2O_3 prepared at the lowest decomposition temperature of each iron salt gives the greatest promoting effect on the decomposition of $KClO_4$.

Figure 6 shows the relation between the preparation temperature of α-Fe_2O_3 and the specific surface area. The surface area of three series of α-Fe_2O_3 decreases with increasing preparation temperature, and the values decrease to less than $2\,m^2\,g^{-1}$ by the calcination at temperatures above 1000°C. In Fig. 7, the crystalline size of α-Fe_2O_3 is plotted as a function of its preparation temperature. It is seen that the crystalline size increases with the preparation temperature. From Figs. 6 and 7, it is assumed that α-Fe_2O_3 prepared at a low temperature has a low crystallinity and is highly defective. On the other hand, all α-Fe_2O_3 samples prepared at high temperatures, above 1000°C, are considered to have similar properties regardless of the starting materials. Figure 8 indicates the relation between the crystalline size of α-Fe_2O_3 and the initial decomposition temperature (T_i). As shown by the broken

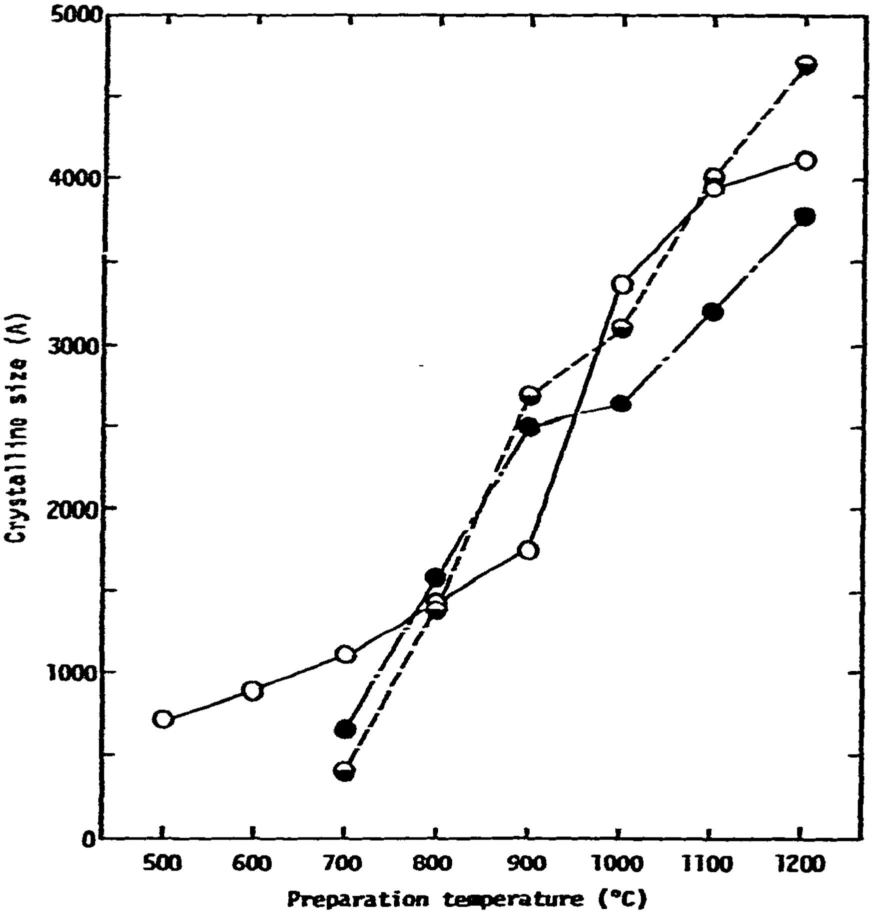

Fig. 7. Relation between crystalline size and preparation temperature of α-Fe_2O_3. ○, α-Fe_2O_3(A); ●, α-Fe_2O_3(S_1); ⊖, α-Fe_2O_3(S_2).

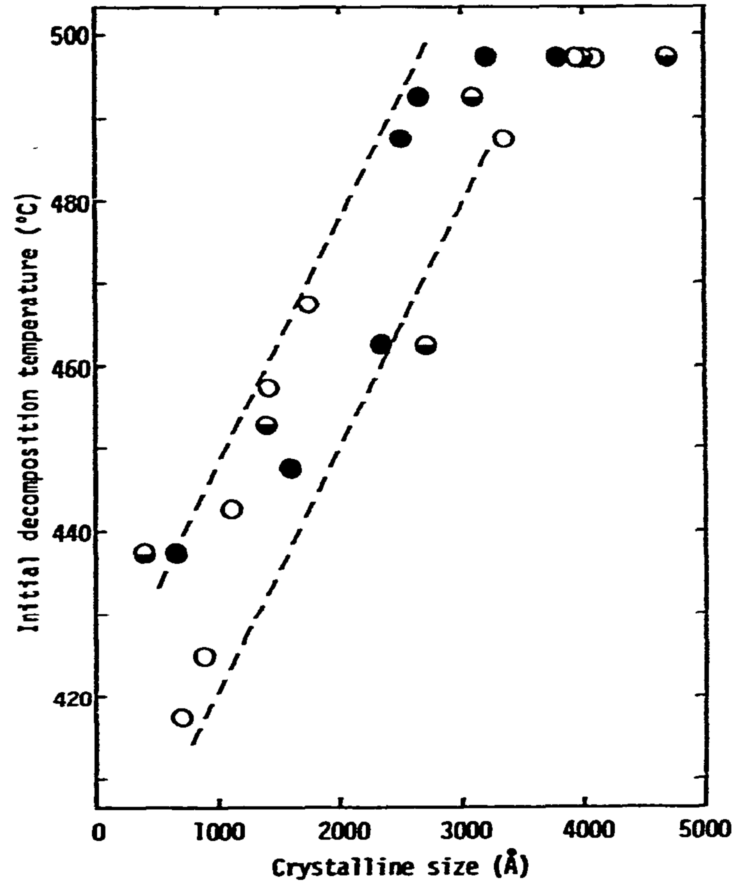

Fig. 8. Relation between crystalline size and initial decomposition temperature (T_i). ○, α-Fe_2O_3(A); ●, α-Fe_2O_3(S_1); ⊖, α-Fe_2O_3(S_2).

line, the values of T_i have a tendency to increase with an increase in the crystalline size, and the oxides with a crystalline size above 3000 Å tend to give the same values for T_i.

DISCUSSION

It is found that the catalytic activity of α-Fe_2O_3 for the thermal decomposition of $KClO_4$ is related to the preparation temperatures rather than the kind of starting iron salts.

The thermal decomposition reaction of $KClO_4$ proceeds according to eqns (1) and (2) in which Cl^{7+} is reduced to Cl^{5+} and Cl^-, and O^{2-} is oxidized to O_2. It is assumed, therefore, that the decomposition involves the electron transfer process.

As shown in the previous paper[11], the metal oxides with high electrical conductivity markedly promoted the thermal decomposition of $KClO_4$, and the promoting action by the oxides was considered to be related to both the electrical conductivity and the oxygen abstraction power, and the following scheme was proposed for n-type semiconductive oxide.

$$2e^-_{(oxide)} + ClO_4^- \rightarrow O^{2-}_{(oxide)} + ClO_3^- \rightarrow 1/2O_2 + ClO_3^- + 2e^-_{(oxide)} \qquad (3)$$

where, $e^-_{(oxide)}$ = electron of conduction band of oxide, $O^{2-}_{(oxide)}$ = oxygen ion abstracted by oxide.

Eqn (3) shows that the oxide promotes the transfer of electrons and the abstraction of oxygen of ClO_4^- simultaneously.

α-Fe_2O_3 is usually classified[20, 21] as an n-type semiconductive oxide. The donor center in the oxide is provided by the excess Fe^{2+} ions, which ionizes to Fe^{3+} to give the conduction electron. It is considered that the concentration of the Fe^{2+} ion in α-Fe_2O_3 varies with the preparation temperature. Especially, α-Fe_2O_3 prepared by the decomposition of $Fe(OH)(CH_3COO)_2$ at low temperatures, which were observed to have low crystallinity, may have a high concentration of Fe^{2+} ions, since the decomposition proceeds through Fe_3O_4 in an early stage. On the other hand, Okamoto et al.[22] estimated that the hydrous ferric oxide with low crystallinity has a low ionization energy of Fe^{2+} and a large specific surface area. Accordingly, it is considered that the high catalytic activity of α-Fe_2O_3 prepared at a low temperature is due to the high concentration of Fe^{2+} ions with low ionization energy. These Fe^{2+} ions in the oxide may give electrons even at a low temperature, which leads to the promotion of the decomposition of $KClO_4$ shown by eqn (3).

REFERENCES

1 P. K. Gallagher, D. W. Johnson, Jr., F. Schrey and D. J. Nitti, *Am. Ceram. Soc. Bull.*, 52 (1973) 842.
2 F. Solymosi, K. Jáky and Z. G. Szabó, *Z. Anorg. Allg. Chem.*, 368 (1969) 211.
3 Y. Mitarai, S. Shirasaki, K. Manabe and T. Kubo, *J. Chem. Soc. Jpn., Ind. Chem. Sect.*, 72 (1969) 1067.
4 V. Balek, *J. Mater. Sci.*, 5 (1970) 714.
5 C. E. Otto and H. S. Fry, *J. Am. Chem. Soc.*, 45 (1923) 1134.
6 E. S. Freeman and D. A. Anderson, *Nature*, 206 (1965) 378.
7 M. M. Markowitz and D. A. Boryta, *J. Phys. Chem.*, 69 (1965) 1114.
8 W. K. Rudloff and E. S. Freeman, *J. Phys. Chem.*, 74 (1970) 3317.
9 M. R. Udupa, *Thermochim. Acta*, 12 (1975) 165.
10 R. Furuichi, T. Ishii and K. Kobayashi, *J. Therm. Anal.*, 6 (1974) 305.
11 M. Shimokawabe, R. Furuichi and T. Ishii, *Thermochim. Acta*, 20 (1977) 347.
12 S. Brunauer and P. H. Emmett, *J. Am. Chem. Soc.*, 59 (1937) 1553.
13 S. Brunauer, P. H. Emmett and E. Teller, *J. Am. Chem. Soc.*, 60 (1938) 309.
14 P. Scherrer, *Göttinger Nachrichten*, 2 (1918) 98.
15 L. Alexander, *J. Appl. Phys.*, 25 (1954) 155.
16 A. E. Harvey, Jr., M. T. Edmison, E. D. Jones, R. A. Seybert and K. A. Catto, *J. Am. Chem. Soc.*, 76 (1954) 3270.
17 A. E. Harvey, Jr., C. J. Wassink, T. A. Rodgers and K. H. Stern, *Ann. N. Y. Acad. Sci.*, 79 (1960) 971.
18 K. H. Stern and M. Bufalini, *J. Phys. Chem.*, 64 (1960) 1781.
19 K. G. Il'in and B. I. Khorunzhii, *Russ. J. Phys. Chem.*, 46 (1972) 838.
20 R. F. G. Gardner, F. Sweett and D. W. Tanner, *J. Phys. Chem. Solids*, 24 (1963) 1175; 24 (1963) 1183.
21 F. J. Morin, *Phys. Rev.*, 83 (1951) 1005; 93 (1954) 1195.
22 G. Okamoto, R. Furuichi and N. Sato, *Electrochim. Acta*, 12 (1967) 1287.